Biochemical and Biophysical Research Communications 408 (2011) 120–125

Contents lists available at ScienceDirect

Biochemical and Biophysical Research Communications

journal homepage: www.elsevier.com/locate/ybbrc

Imaging mass spectrometry reveals characteristic changes in triglyceride and phospholipid species in regenerating mouse liver

Norio Miyamura [a,1], Takashi Nakamura [a,1], Naoko Goto-Inoue [b], Nobuhiro Zaima [b], Takahiro Hayasaka [b], Tokiwa Yamasaki [a], Shuji Terai [c], Isao Sakaida [c], Mitsutoshi Setou [b], Hiroshi Nishina [a,*]

[a] Dept. Developmental and Regenerative Biology, Medical Research Institute, Tokyo Medical and Dental University, Tokyo, Japan
[b] Dept. Molecular Anatomy, Hamamatsu University School of Medicine, Shizuoka, Japan
[c] Dept. Gastroenterology and Hepatology, Yamaguchi University Graduate School of Medicine, Yamaguchi, Japan

ARTICLE INFO

Article history:
Received 25 March 2011
Available online 2 April 2011

Keywords:
Imaging mass spectrometry
Metabolite imaging
Liver regeneration
MALDI-TOF

ABSTRACT

After partial hepatectomy (PH), regenerating liver accumulates unknown lipid species. Here, we analyzed lipids in murine liver and adipose tissues following PH by thin-layer chromatography (TLC), imaging mass spectrometry (IMS), and real-time RT-PCR. In liver, IMS revealed that a single TLC band comprised major 19 TG species. Similarly, IMS showed a single phospholipid TLC band to be major 13 species. In adipose tissues, PH induced changes to expression of genes regulating lipid metabolism. Finally, IMS of phosphatidylcholine species demonstrated distribution gradients in lobules that resembled hepatic zonation. IMS is thus a novel and power tool for analyzing lipid species with high resolution.

1. Introduction

The liver has a remarkable capacity to regenerate after injury [1,2] and partial hepatectomy (PH) in rodents has been useful for investigating the underlying mechanisms. Following PH, hepatocytes in the remaining liver tissue start proliferating such that normal liver mass is restored; the regenerative response is then terminated. To support this hepatocyte proliferation, the liver remnant transiently accumulates lipids that supply the energy and membrane components needed for cell division [3–5]. However, it is unclear what molecular species of lipids are involved and whether PH affects other tissues.

Matrix-assisted laser desorptional/ionization (MALDI) mass spectrometry is often used to analyze low molecular weight compounds such as lipids. A recent refinement called "imaging mass spectrometry" (IMS) allows visualization of the amount and distribution of individual molecular species in tissue sections [6,7]. IMS has successfully revealed changes in lipid identity, amount and distribution in tissue sections of plants and animals [8–11]. In this study, we used IMS to identify lipid species in murine liver regenerating after PH. We also carried out gene expression analysis to define the effects of PH on adipose tissues, which are important for lipid metabolism.

2. Materials and methods

2.1. Reagents

All chemicals used were of the highest purity, including trifluoroacetic acid (TFA) and methanol (Kanto Chemical, Japan) and 2,5-dihydroxybenzoic acid (DHB) (Bruker Daltonics, Germany). Ultrapure water from a Milli-Q system (Millipore, USA) was used for all buffers and solvents.

2.2. Animals

Female C57BL/6J mice (10 weeks old; CLEA Japan Inc.) were kept in a temperature-controlled room with a 12 h dark/light cycle and fed CE-2 diet (CLEA). PH or sham surgery was performed as described [12] between 9 and 10 a.m. and animals were sacrificed at 0, 6, 12 or 24 h post-operation. All animal experiments were conducted according to the guidelines of Tokyo Medical and Dental University.

Abbreviations: BAT, brown adipose tissue; CE, cholesterol ester; Chol, cholesterol; DG, diacylglycerol; FA, fatty acid; FFA, free fatty acids; IMS, imaging mass spectrometry; LPC, lysophosphatidylcholine; MALDI-TOF, matrix-assisted laser desorptional ionization-time of flight; PC, phosphatidylcholine; PE, phosphatidylethanolamine; PH, partial hepatectomy; PI, phosphatidylinositol; PS, phosphatidylserine; SM, sphingomyelin; SCF, subcutaneous fat; TG, triglyceride; VF, visceral fat.

* Corresponding author. Address: 1-5-45 Yushima, Bunkyo-ku, Tokyo 113-8510, Japan. Fax: +81 3 5803 5829.
E-mail address: nishina.dbio@mri.tmd.ac.jp (H. Nishina).

[1] These authors contributed equally to this work as first authors.

0006-291X/$ - see front matter © 2011 Elsevier Inc. All rights reserved.
doi:10.1016/j.bbrc.2011.03.133

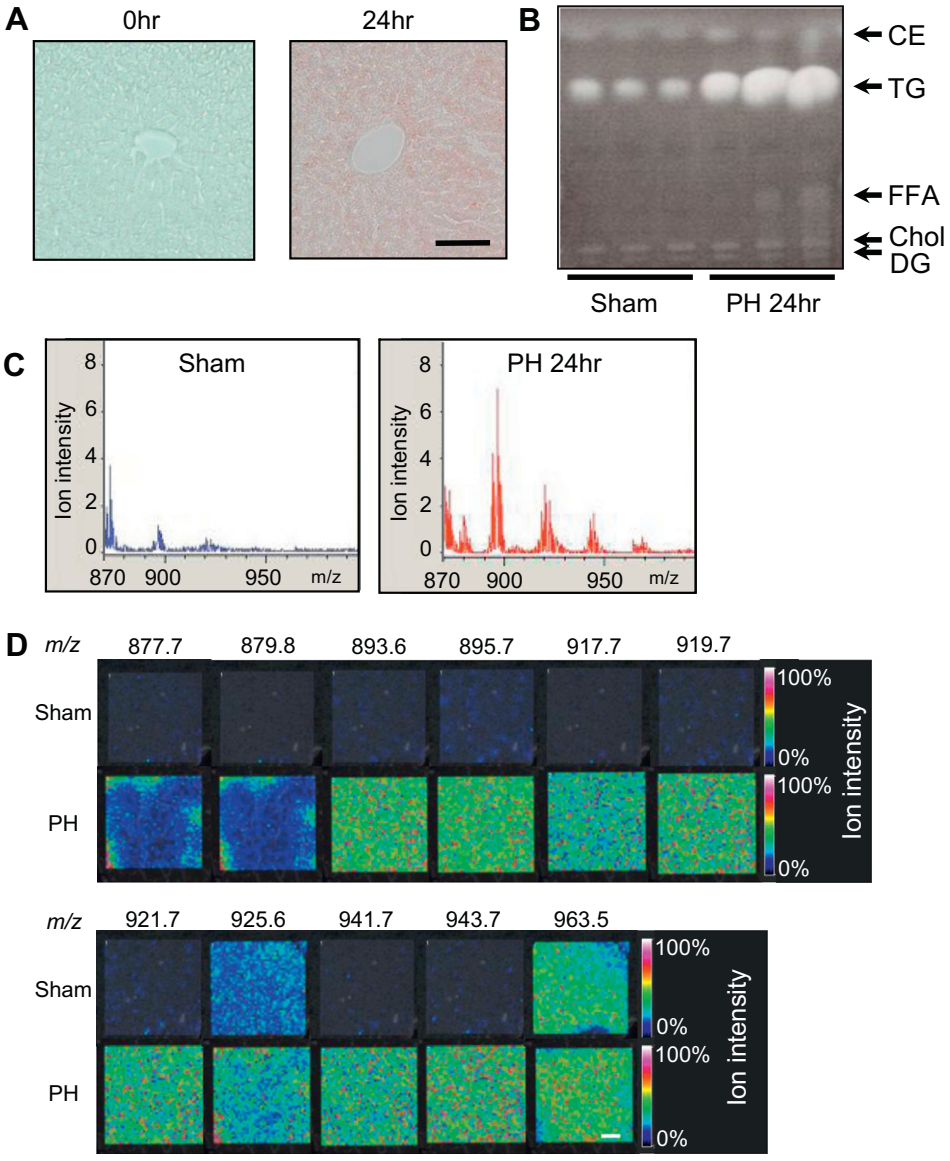

Fig. 1. Dramatic changes of multiple triglyceride species in concentration during liver regeneration. (A) Oil red O-stained liver sections showing increased TG (red) globules in hepatocytes at 24 h post-PH. Scale bar, 100 μm. (B) TLC of neutral lipids in liver extracts from mice at 24 h post-PH or sham surgery. For all experiments, results shown are representative of 3 mice/group. (C) MALDI-TOF average mass spectra of liver from mice at 24 h post-PH or sham surgery. A range from 875 *m/z* to 1000 was examined. (D) MALDI-TOF-MS imaging of lipid ion species in liver sections from the mice in (C). Scale bar, 500 μm.

2.3. Oil red O staining

Frozen liver sections were prepared using O.C.T Compound (Sakura Finetek, Japan) and a cryostat (CM 1950; Leica Microsystems, Germany) set to 10 μm. Oil red O staining was performed as described [13].

2.4. Lipid extraction and thin-layer chromatography

Liver lipids were extracted using chloroform:methanol (2:1) as described [14]. For TLC, Silica Gel 60 plates (Merck, USA) were run in n-hexane:diethyl ether:acetic acid (80:30:1) to separate neutral lipids, and in methyl acetate:propanol:chloroform:methanol:0.2% KCl (25:25:25:10:9) to resolve phospholipids. Lipids were visualized using primuline (Nakarai Tesque, Japan) and identified based on migration compared to standards [15].

2.5. Quantitative real-time RT-PCR

Quantitative real-time RT-PCR was performed as described [16]. Primer sequences are listed in Supplementary Information (Table S1).

2.6. IMS samples

IMS samples were prepared as previously described [10,17] with a slight modification. Frozen liver cryostat sections (8 μm) were mounted on indium-tin-oxide-coated glass slides (Bruker Daltonics). DHB matrix solution (50 mg/ml DHB in 70% methanol/0.1% TFA) was sprayed uniformly over mounted sections with a 0.2 mm nozzle airbrush (Mr. Hobby, Japan).

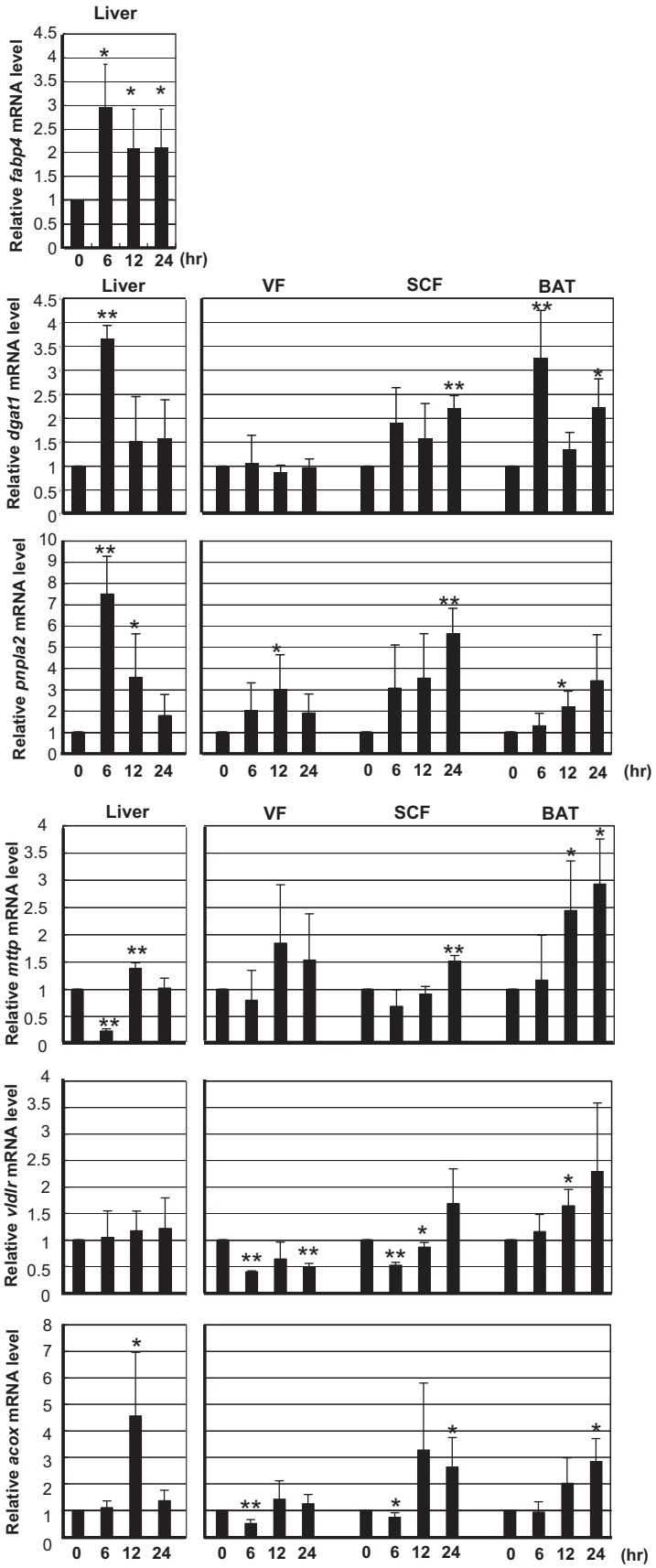

Fig. 2. mRNA levels of the indicated TG metabolism-related and β-oxidation-related genes in liver, visceral fat, subcutaneous fat and BAT. Data are mean fold induction ± SD relative to *gapdh*. $n = 3$ $^{*}p < 0.05$, $^{**}p < 0.01$ vs. value at 0 h.

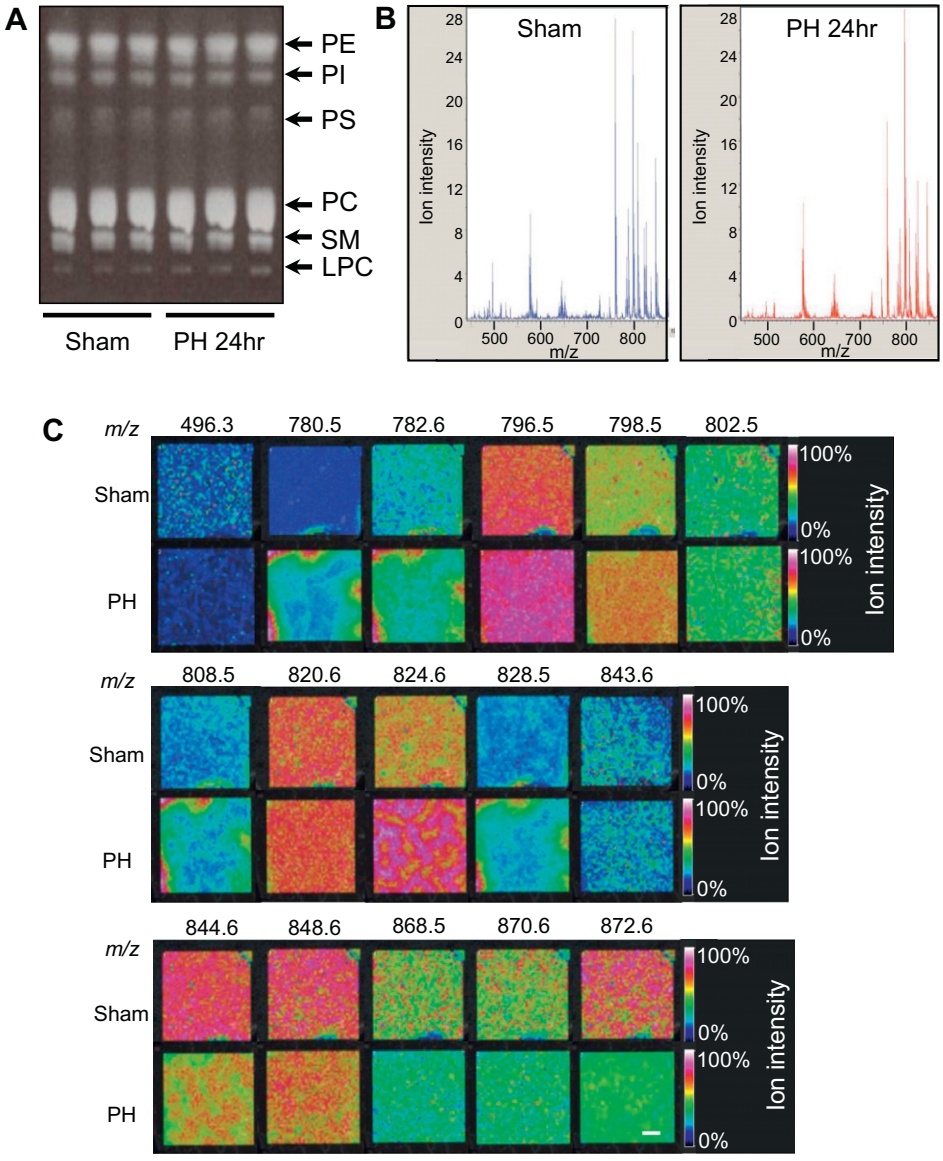

Fig. 3. The existence and dynamic distribution of clearly multiple phospholipids. (A) TLC of phospholipids in liver extracts from mice at 24 h post-PH or sham surgery. (B) MALDI-TOF mass spectra of liver extracts from mice at 24 h post-PH or sham surgery. A range from 440 *m/z* to 875 was examined. (C) MALDI-TOF-MS imaging of lipid ion species in liver sections from the mice in (B). Scale bar, 500 μm.

2.7. MALDI-TOF IMS

MALDI mass spectrometry was performed using an Ultraflex II TOF/TOF instrument (Bruker Daltonics) equipped with a 355 nm Nd:YAG laser with a 200 Hz repetition rate. The measurement pitch was 50 μm. Data were acquired in positive-ion mode using an external calibration method. Mass spectrometer parameters were set to obtain *m/z* values of 400–2000. All spectra were acquired automatically with FlexImaging software (Bruker Daltonics). The laser was irradiated 200 times per position. Peaks were normalized to total ion current and compared. The Lipid Search (http://lipid-search.jp) database were used to determine lipid molecular species.

3. Results

3.1. Multiple triglyceride species in regenerating liver

Oil red O staining of hepatocytes in regenerating liver at 24 h post-PH revealed an accumulation of TG that did not appear in sham-treated livers (Fig. 1A). TLC of extracted total lipids from these livers revealed bands of CE, TG, FFA, Chol and DG that were increased or unchanged in extracts from PH livers (Fig. 1B). IMS analysis of liver sections at 24 h after sham treatment or PH revealed increases in PH livers of several peaks in the mass range from *m/z* 875 to *m/z* 1000 (Fig. 1C), 19 of which represented abundant TG molecular species (Table S2). The visualization of these data shown in Fig. 1D confirms that multiple TG species undergo dramatic changes in concentration during liver regeneration.

3.2. Changes to expression of lipid-related genes in regenerating liver and adipose tissues

Because adipose tissues are vital for lipid metabolism, we investigated whether PH affected these tissues as well as the liver. We examined gene expression patterns in liver, visceral fat (VF), subcutaneous fat (SCF) and brown adipose tissue (BAT) of animals subjected to PH or sham surgery. Specifically, we monitored the expression of *fabp4*, which encodes FFA binding protein and served

as a positive control; *dgat*, encoding an enzyme catalyzing the final stage of TG synthesis; *pnpla2,* encoding an enzyme catalyzing the first step in TG hydrolysis; *mttp*, encoding a protein involved in β-lipoprotein production; *vldlr*, important for the metabolism of apoprotein-E-containing TG-rich lipoproteins; and *acox*, encoding the first enzyme of the FA β-oxidation pathway. The mRNA levels of these genes as determined by real-time RT-PCR were normalized to the internal controls *gapdh* (Fig. 2) and *tubb2b* (data not shown), yielding similar results. Consistent with a previous report [18], *fabp4* was upregulated in regenerating liver, showing its highest induction at 6 h post-PH. The same pattern held true for upregulation of *dgat* and *pnpla2*, with *acox* peaking at 12 h post-PH. In contrast, *mttp* was downregulated at 6 h post-PH but upregulated over control levels by 12 h post-PH. The level of liver *vldlr* mRNA was not altered by PH. For *dgat1*, *pnpla2* and *acox*, mRNA levels had returned to baseline by 24 h post-PH. Interestingly, different expression patterns were observed in adipose tissues. At 6 h post-PH, *dgat1* mRNA was upregulated only in BAT whereas *pnpla2* tended to be upregulated only after 12 h post-PH. Unlike its pattern in liver, *mttp* mRNA was not downregulated in adipose tissues and steadily rose after 12 h post-PH. Levels of *vldlr*, which were unchanged in liver, were downregulated in VF. *Acox* mRNA was upregulated over control levels in SCF and BAT by 24 h post-PH. These results indicate that PH induces striking changes to lipid-related gene expression patterns in adipose tissues.

3.3. Phospholipids in regenerating liver

Phospholipids are a major component of all cell membranes and are important for liver regeneration. TLC of liver extracts from our PH- or sham-treated mice revealed equivalent bands of PE, PI, PS, PC, SM and LPC (Fig. 3A). IMS performed at 24 h post-PH or sham surgery showed several peaks in the mass range from *m/z* 440 to *m/z* 875 that were present in both PH liver and sham-treated liver (Fig. 3B). Of these, 11 were assigned by their masses to abundant PC molecular species, one to LPC and one to sphingomyelin (Table 1). Compared to sham-treated liver, levels of six putative PC species such as PC (1-acyl 34:2) and PC (1-acyl 36:5) and one sphingomyelin were increased in regenerating liver, whereas one putative LPC and two putative PC species were decreased. The IMS visualization of these molecular species shown in Fig. 3C clearly demonstrates the differences in levels of liver phospholipid species between PH- and sham-treated mice. In particular, the perivenous area of the sham-treated liver displayed lower levels of *m/z* 848.6 but higher levels of *m/z* 796.5 compared to periportal area. These results show that levels of phospholipid species change dynamically following PH, and that several of these species show a gradient in their intralobular distribution that is reminiscent of hepatic zonation [19].

Table 1
Changes to phospholipid species in post-PH liver sections as determined by MALDI-TOF-MS.

m/z	Change*	Putative molecular species
496.3	↓	LPC(16:0)
780.5	↑	PC(1-acyl 34:2) + Na
782.6	↑	PC(1-acyl 34:1) + Na
796.5	↑	PC(1-acyl 34:2) + K
798.5	↑	PC(1-acyl 34:1) + K
802.5	↑	PC(1-acyl 36:5)
808.5	↑	PC(1-acyl 36:2) + Na
820.6	→	PC(1-acyl 36:4)
824.6	↑	PC(1-acyl 36:2) + K
828.5	↑	PC(1-acyl 36:0)
843.6	↑	SM(2-amido22:2)
844.6	↑	PC(1-acyl 38:6)
848.6	→	PC(1-acyl 38:4)
868.5	↓	PC(1-acyl 40:8)
870.6	→	PC(1-acyl 40:7)
872.6	↓	PC(1-acyl 40:6)

↑, increase; ↓, decrease; →, unchanged; SM, sphingomyelin.
* Change relative to sham surgery.

4. Discussion

In this study, we have demonstrated that IMS can uncover previously hidden lipid species in regenerating liver after PH. We have also shown that PH not only affects liver lipids but also the expression of lipid-related genes in adipose tissues. The most common method used to analyze lipids in post-PH liver is TLC, which in our hands detected only a single band of TG that increased with time, as well as a collection of single phospholipid bands that did not change in intensity (Figs. 1B and 3A). In contrast, IMS revealed the existence and dynamic distribution of clearly multiple TGs (Fig. 1C and D, Table S2) and phospholipids (Fig. 3B and C, Table 1). Our results therefore demonstrate that IMS is a highly useful tool for both analyzing lipid species with high resolution.

Our results also show that PH affects the expression of genes that regulate TG synthesis, degradation and β-oxidation in adipose tissues (Fig. 2). Although adipose tissues are not directly connected to liver, they synthesize and release TGs that can travel in the blood to this organ. We propose that the injured liver may send an unidentified signal to the adipose tissues that regulates lipid metabolism. One possible route for such a signal might be via the blood. Indeed, it was recently reported that the serum total TG concentration was decreased by 75% at 6 h post-PH in mice [18]. The altered gene expression we observed in adipose tissues post-PH could result from cellular sensing of a reduction in blood TG. Another possibility may be signal transmission via the central nervous system (CNS). Imai et al. recently reported that hepatic ERK activation regulates pancreatic beta cell mass via the CNS [20]. Thus, following PH, hepatocytes may transmit a neural signal to adipose tissues that communicates their need to acquire more lipids for regeneration. Because the liver is a central metabolic regulator, interactions between the liver and other tissues mediated through the blood and/or CNS may be essential for whole body homeostasis.

Moreover, IMS allowed the 2D-visualization of TG and phospholipid distribution patterns in liver (Figs. 1D and 3C). Hepatic zonation refers to a gradient of molecules that appears from the perivenous region of a liver lobule to its periportal region [19]. We found that the perivenous area of the sham-treated liver displayed lower levels of *m/z* 848.6 but higher levels of *m/z* 796.5 compared to periportal area (Fig. 3C), consistent with hepatic zonation. Although a few previous studies have provided evidence of differential distribution of some mRNAs and proteins in liver lobules as determined by *in situ* hybridization and immunostaining, our IMS analysis is the first to show that small molecules such as lipids also exhibit hepatic zonation.

Increased fat content (steatosis) is a common feature of a liver under stress, be it due to regeneration after PH, or to altered function due to severe fasting. Prior to our study, it was not clear whether these fatty livers differed in their lipid content. Zaima et al. and van Ginneken et al. reported that PC (1-acyl 34:2) was the dominant lipid species increasing in the pathologic fatty liver induced in fasting mouse and rat models [21,22]. These groups therefore proposed that PC (1-acyl 34:2) is important for the evolution of fatty liver in this context. In our study, we too observed an increase in PC (1-acyl 34:2) in regenerating liver post-PH (Table 1). However, we also detected elevations in additional lipid species such as PC (1-acyl 36:5), which was decreased in fasting liver

[21,22]. PC (1-acyl 36:5) may therefore be a biomarker specific for steatosis induced by PH. Thus, MS and IMS are powerful tools that can assist in the detailed measurement of lipid metabolism.

Acknowledgments

This work was supported in part by research grants from the Ministry of Education, Culture, Sports, Science and Technology of Japan, the Ministry of Health, Labour and Welfare of Japan, and the Japan Society for the Promotion of Science.

Appendix A. Supplementary data

Supplementary data associated with this article can be found, in the online version, at doi:10.1016/j.bbrc.2011.03.133.

References

[1] G.K. Michalopoulos, M.C. DeFrances, Liver regeneration, Science 276 (1997) 60–66.
[2] S. Hata, M. Namae, H. Nishina, Liver development and regeneration: from laboratory study to clinical therapy, Development Growth and Differentiation 49 (2007) 163–170.
[3] T.J. Delahunt, D. Rubinste, Accumulation and release of triglycerides by rat liver following partial hepatectomy, Journal of Lipid Research 11 (1970) 536.
[4] A.B. Murray, W. Strecker, S. Silz, Ultrastructural-changes in rat hepatocytes after partial-hepatectomy, and comparison with biochemical results, Journal of Cell Science 50 (1981) 433–448.
[5] E.A. Glende, W.S. Morgan, Alteration in liver lipid and lipid fatty acid composition after partial hepatectomy in rat, Experimental and Molecular Pathology 8 (1968) 190.
[6] M. Stoeckli, P. Chaurand, D.E. Hallahan, R.M. Caprioli, Imaging mass spectrometry: a new technology for the analysis of protein expression in mammalian tissues, Nature Medicine 7 (2001) 493–496.
[7] M. Stoeckli, T.B. Farmer, R.M. Caprioli, Automated mass spectrometry imaging with a matrix-assisted laser desorption ionization time-of-flight instrument, Journal of the American Society for Mass Spectrometry 10 (1999) 67–71.
[8] T. Harada, A. Yuba-Kubo, Y. Sugiura, N. Zaima, T. Hayasaka, N. Goto-Inoue, M. Wakui, M. Suematsu, K. Takeshita, K. Ogawa, Y. Yoshida, M. Setou, Visualization of volatile substances in different organelles with an atmospheric-pressure mass microscope, Analytical Chemistry 81 (2009) 9153–9157.
[9] S. Shimma, Y. Sugiura, T. Hayasaka, N. Zaima, M. Matsumoto, M. Setou, Mass imaging and identification of biomolecules with MALDI-QIT-TOF-based system, Analytical Chemistry 80 (2008) 878–885.
[10] N. Goto-Inoue, T. Hayasaka, Y. Sugiura, T. Taki, Y.T. Li, M. Matsumoto, M. Setou, High-sensitivity analysis of glycosphingolipids by matrix-assisted laser desorption/ionization quadrupole ion trap time-of-flight imaging mass spectrometry on transfer membranes, Journal of Chromatography B-Analytical Technologies in the Biomedical and Life Sciences 870 (2008) 74–83.
[11] N. Zaima, T. Hayasaka, N. Goto-Inoue, M. Setou, Imaging of metabolites by MALDI mass spectrometry, Journal of Oleo Science 58 (2009) 415–419.
[12] C. Mitchell, H. Willenbring, A reproducible and well-tolerated method for 2/3 partial hepatectomy in mice, Nature Protocols 3 (2008) 1167–1170.
[13] E. Shteyer, Y.J. Liao, L.J. Muglia, P.W. Hruz, D.A. Rudnick, Disruption of hepatic adipogenesis is associated with impaired liver regeneration in mice, Hepatology 40 (2004) 1322–1332.
[14] J. Folch, M. Lees, G.H.S. Stanley, A simple method for the isolation and purification of total lipides from animal tissues, Journal of Biological Chemistry 226 (1957) 497–509.
[15] N. Goto-Inoue, T. Hayasaka, T. Taki, T.V. Gonzalez, M. Setou, A new lipidomics approach by thin-layer chromatography-blot-matrix-assisted laser desorption/ionization imaging mass spectrometry for analyzing detailed patterns of phospholipid molecular species, Journal of Chromatography A 1216 (2009) 7096–7101.
[16] J. Seo, Y. Asaoka, Y. Nagai, J. Hirayama, T. Yamasaki, M. Namae, S. Ohata, N. Shimizu, T. Negishi, D. Kitagawa, H. Kondoh, M. Furutani-Seiki, J.M. Penninger, T. Katada, H. Nishina, Negative regulation of wnt11 expression by Jnk signaling during zebrafish gastrulation, Journal of Cellular Biochemistry 110 (2010) 1022–1037.
[17] S. Taira, Y. Sugiura, S. Moritake, S. Shimma, Y. Ichiyanagi, M. Setou, Nanoparticle-assisted laser desorption/ionization based mass imaging with cellular resolution, Analytical Chemistry 80 (2008) 4761–4766.
[18] E.P. Newberry, S.M. Kennedy, Y. Xie, J. Luo, S.E. Stanley, C.F. Semenkovich, R.M. Crooke, M.J. Graham, N.O. Davidson, Altered hepatic triglyceride content after partial hepatectomy without impaired liver regeneration in multiple murine genetic models, Hepatology 48 (2008) 1097–1105.
[19] K. Jungermann, Zonation of metabolism and gene expression in liver, Histochemistry and Cell Biology 103 (1995) 81–91.
[20] J. Imai, H. Katagiri, T. Yamada, Y. Ishigaki, T. Suzuki, H. Kudo, K. Uno, Y. Hasegawa, J.H. Gao, K. Kaneko, H. Ishihara, A. Niijima, M. Nakazato, T. Asano, Y. Minokoshi, Y. Oka, Regulation of pancreatic beta cell mass by neuronal signals from the liver, Science 322 (2008) 1250–1254.
[21] N. Zaima, Y. Matsuyama, M. Setou, Principal component analysis of direct matrix-assisted laser desorption/ionization mass spectrometric data related to metabolites of fatty liver, Journal of Oleo Science 58 (2009) 267–273.
[22] V. van Ginneken, E. Verhey, R. Poelmann, R. Ramakers, K.W. van Dijk, L. Ham, P. Voshol, L. Havekes, M. Van Eck, J. van der Greef, Metabolomics (liver and blood profiling) in a mouse model in response to fasting: a study of hepatic steatosis, Biochimica et Biophysica Acta (BBA) – Molecular and Cell Biology of Lipids 1771 (2007) 1263–1270.